SECONDARY PARTICLE PRODUCTION AND CAPTURE FOR MUON ACCELERATOR APPLICATIONS

S.J. Brooks*, RAL, Oxfordshire OX11 0QX, UK

Abstract

Intense pulsed muon beams are required for projects such as the Neutrino Factory and Muon Collider. It is currently proposed to produce these from a high-Z target using a multi-megawatt proton driver. This paper examines the effect of proton energy on the yield and distribution of particles produced from tantalum and mercury, with further analysis using a tracking code to determine how these distributions will behave downstream, including a breakdown of loss mechanisms. Example 'muon front end' lattices are used from the UK Neutrino Factory design.

PARTICLE PRODUCTION TARGET

The target is cylindrical with radius fixed at 1 cm while the length is varied in proportion to the hadronic interaction length as shown in table 1. To improve comparability between particle production runs, a datum of 20 cm length in the tantalum target was chosen, which sets the scale for the rest. The origin of the 20 cm figure was a previous study showing only small gains (<20%) in production for any longer target. Use of these figures as near-optimal values is supported by a separate study of the US Study II beamline in which 60 cm was found to be the best length for a graphite target [1].

Table 1: L_h is the hadronic interaction length as given by http://www.slac.stanford.edu/comp/physics/matprop.html

Element	Z	L_h (cm)	Equivalent to 20 cm Ta
Ta	73	11.18	20cm
Hg	80	13.95	25cm
C	6	36.92	66cm
Cu	29	15.16	27cm
W	74	9.54	17cm
Mo	42	14.96	27cm

The incident proton beam is modelled as having a circular parabolic distribution with no angular spread. This is essentially a 4D 'waterbag' distribution in the limit of low angular divergence. The protons travel in a direction parallel to the axis of the cylinder and where longitudinal distribution is important are given a 1 ns RMS time spread.

This simple target set-up was run in the code MARS15 [2] to generate particle distributions leaving the target surface for a range of different proton energies. These data provide the input distributions for tracking of muon capture systems downstream.

One issue with this method is that the full MARS particle production simulation is only run up to the surface of the rod, and magnetic fields in the region outside can cause particles to spiral back and re-enter it later on. MARS is not run on a larger section of beamline because this way optimisation of the surrounding magnetic fields as described in [3] can be conducted independently of the particle generation, since the magnetic field has been found to have a negligible effect on particle paths within the target [4]. The main concern is that pions may be re-absorbed in the target material, and this effect may be aggravated by extending the length of the target as necessary in the case of low Z. An approximation to the full model is to assume that pions have a characteristic 'absorption length' in the target material, according to which they will be lost in an exponential fashion, assuming they are only converted into particles which are no longer of interest.

Table 2: Calculations show an absorption length of ≈10 cm for pions at the energies of interest.

Pion energy	$L_{\mathrm{Absorb}}(\pi^+)$ (cm)	$L_{\mathrm{Absorb}}(\pi^-)$ (cm)
0.1 GeV	8.21	6.47
0.3 GeV	10.66	10.62
1 GeV	13.90	15.87

To estimate this absorption length, some simulations were run in MARS where the incident beam was of pions rather than protons. Energies of 0.1, 0.3 and 1 GeV were used the reflect the lower energies typical of the secondary particles and tantalum for the material. The derived absorption lengths are shown in table 2.

PHASE-ROTATION BEAMLINE

The target is enclosed in a 20 T solenoid, radius 10 cm, which is followed by a 30 m pion to muon decay channel of ≈4 T solenoids with 40 cm radius. This channel and everything that follows was derived from an optimisation of all component parameters for mesons from a 10 GeV proton beam on tantalum, using methods discussed in [3]. The remainder of the beamline (the *phase rotator*) has the goal of reducing the spread of energies in the beam until as many muons as possible lie within the band 180 ± 23 MeV, the design energy acceptance of the Rees cooling ring [5].

* s.j.brooks@rl.ac.uk

The phase rotator has a solenoidal focussing system at ≈3 T with only 15 cm radius. The bore is smaller than the previous section as the solenoids are interleaved with 31.4285 MHz RF cavities with a 15 cm aperture. There are 30 of these cells with 2.2 MV on each cavity, which rotate the longitudinal phase-space as shown in figure 1.

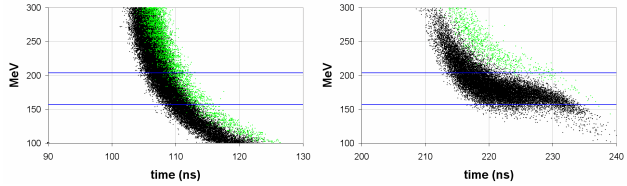

Figure 1: Longitudinal phase space before and after the phase rotator. Pions are green.

RESULTS

The pions, muons and kaons generated by the MARS15 simulations were used as input for running the particle tracking code `Muon1` up to the end of phase rotation. Tantalum was used as the target material until otherwise stated.

Transmission with Proton Energy

The maximum transmission of 0.00343 μ^+/(p.GeV) was attained using a proton energy of 8 GeV and this decreases monotonically above that, as shown by the lowest stripe in figure 2 (see also figure 7). For lower energies the yield decreases until 3.25 GeV but then starts to rise again. The graph also shows that the type of phase rotation employed only works for one sign: the proportion of μ^- falling within the energy band is much lower because they have been rotated in the wrong direction in longitudinal phase space, increasing their energy spread as shown in figure 4.

Figure 3 shows that there is little variation in the efficiency of energy capture as the input proton energy changes.

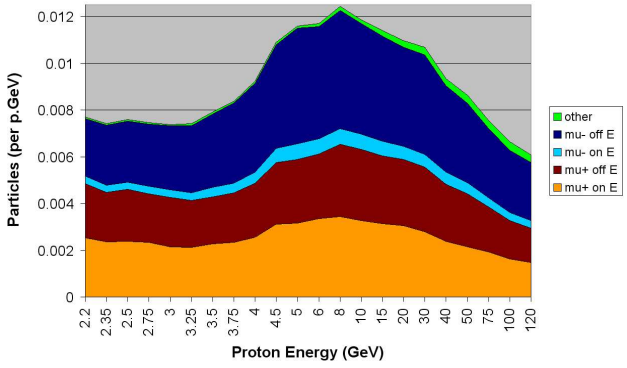

Figure 2: Yield of particles leaving the phase rotation channel (p.GeV is a unit of beam power).

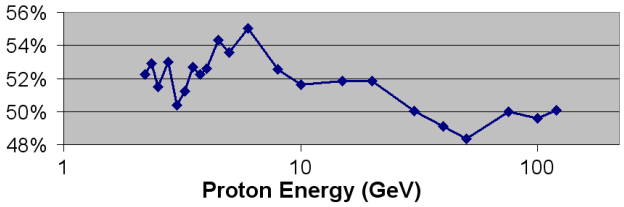

Figure 3: Fraction of transmitted μ^+ falling within the required energy band.

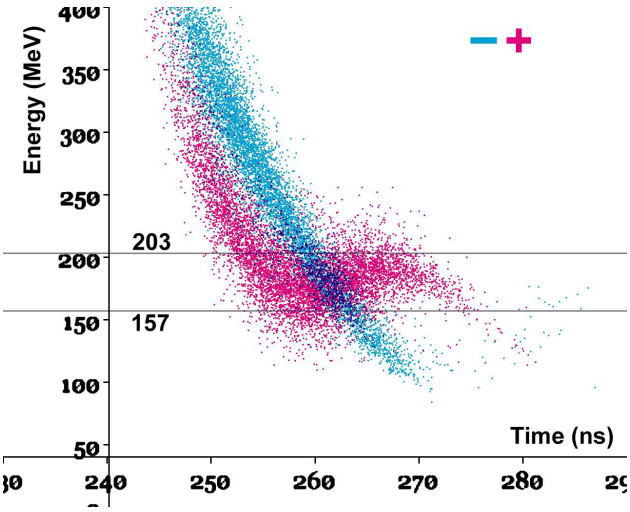

Figure 4: Longitudinal phase space of μ^+ (pink) and μ^- (blue) leaving the phase rotator for the 8 GeV case.

Redistribution of Losses

Beam losses were counted for each proton energy and categorised into ten different types, in terms of mechanism and location, as shown in figure 5. The main trend is that losses move further down the decay channel as proton energy increases, which can be attributed to high-p_T pions being forward boosted, making them more parallel to the beamline axis while still uncapturable by the fields in the channel.

Muon Sign Effects

The sign ratio μ^-/μ^+ was examined both as a ratio of on-energy muons and of any muons reaching the end of the channel (see figure 6). At low energies μ^+ are more successful, with only 0.63 times as many μ^- finishing on-energy from 2.2 GeV protons, though this effect rapidly becomes less significant until the signs are equivalent at 3.75 GeV. This stays the case until at $\geq$40 GeV there is a slight excess of μ^-, reaching a ratio of 1.14 above the positives by 120 GeV.

It was found that for proton energies of 3.5–40 GeV, all loss mechanism fractions differed by relatively less than 6% between the signs. At lower energies, 8–20% more μ^- were lost in the late phase rotation channel and 11–26% fewer reached the end of the channel successfully,

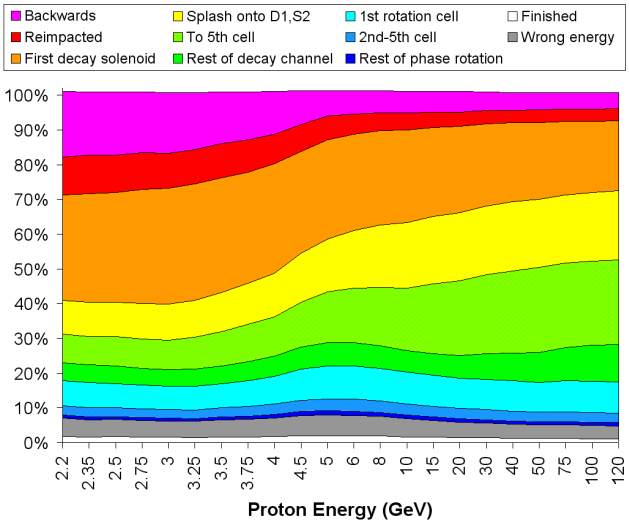

Figure 5: Loss types as a fraction of particle count. The sum is slightly more than 100% due to decays such as $K^+ \to \pi^+\pi^+\pi^-$.

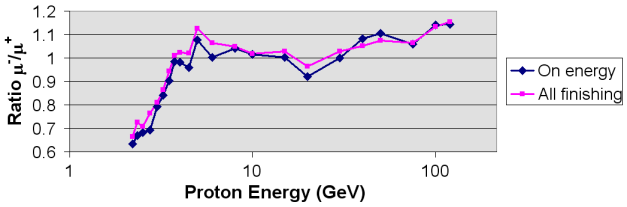

Figure 6: Performance of negative compared to positive muons.

whereas at the highest energies the finishing fraction for μ^- was slightly higher (by about 9%). Note that these figures are ratios between loss *fractions* and so independent of bulk production excesses in either sign: they are caused by changes in the particle distribution itself.

Differences between Tantalum and Mercury

The original tantalum rod was replaced by a mercury one with length as in table 1 and the first solenoid was extended by the same amount to accomodate it. Yields (for μ^+) are compared to tantalum in figure 7. The largest yield was 0.00312 μ^+/(p.GeV) at 15 GeV, with similar values extending down to 6 GeV. Mercury is generally equal with tantalum at $\geq$15 GeV but loses by as much as 20% once below 5 GeV, despite a 1–5% advantage in raw meson production at the target surface.

Carbon Target Behaviour

Figure 7 shows that carbon has a different energy dependency to the high-Z materials, mainly in line with its production cross-section. The carbon target is much longer than the others and it is natural to wonder if this increasing source length affects longitudinal behaviour downstream. The percentages of μ^+ that leave the phase rotator on-

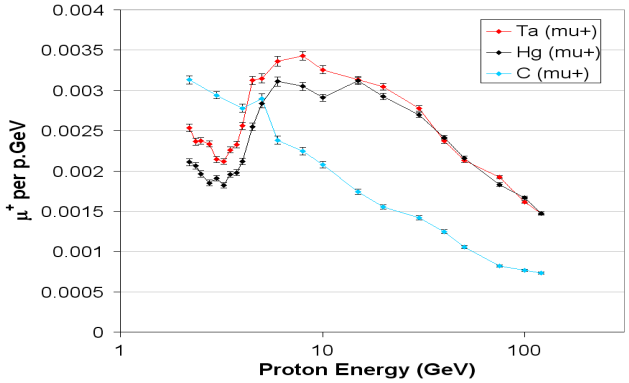

Figure 7: Performance of Ta, Hg and C targets. Error bars are 1σ in Monte Carlo statistics.

energy are 48–55%, 43–47% and 21–29%, respectively, for Ta, Hg and C at any energy examined. This is roughly a decrease of 1% for every 1 cm of target length added!

Cross-Optimisation with 2.2 GeV

Another phase rotation lattice was available that had been optimised using the same method for a pion distribution from a 2.2 GeV beam instead of a 10 GeV one. This was run at both energies and the μ^+ yields compared to those of the original lattice in table 3.

Table 3: μ^+/(p.GeV) yields of 'cross-optimised' phase rotation lattices.

Proton Energy	**2.2 GeV lattice**	**10 GeV lattice**
2.2 GeV	0.00240	0.00253
10 GeV	0.00310	0.00326

An examination of the parameters indicated that little was different between the two lattices and the 10 GeV one had converged better during optimisation, which has lead to its slightly higher results than the other here. There is no sign that the optimal lattice depends in any significant way on the pion distribution at these energies.

REFERENCES

[1] H.G. Kirk, BNL, private communication.

[2] N.V. Mokhov, "The Mars Code System User's Guide", Fermilab-FN-628 (1995); N.V. Mokhov, "Status of MARS Code", Fermilab-Conf-03/053 (2003); N.V. Mokhov, K.K. Gudima, C.C. James et al, "Recent Enhancements to the MARS15 Code", Fermilab-Conf-04/053 (2004); http://www-ap.fnal.gov/MARS/.

[3] S.J. Brooks, Quantitative Optimisation Studies of the Muon Front-End for a Neutrino Factory, Proc. EPAC'04.

[4] Supplementary simulation work of the target in a 20T field by J.J. Back, Warwick University.

[5] G.H. Rees *et al.*, Features of a Muon Cooling Ring for a Neutrino Factory, Proc. Nufact'03.